Lead-free piezoelectric ceramics with composition of $(0.97-x)$Na$_{1/2}$Bi$_{1/2}$TiO$_3$-0.03NaNbO$_3$-xBaTiO$_3$

YUGONG WU, HUILI ZHANG, YUE ZHANG, JINYI MA, DAOHUA XIE
School of Electronic and Information Engineering, Tianjin University, Tianjin 300072, People's Republic of China
E-mail: wuyugong@eyou.com

Compositions in (Na$_{1/2}$Bi$_{1/2}$)TiO$_3$ based ternary system, $(0.97 - x)$ (Na$_{1/2}$Bi$_{1/2}$)TiO$_3$-0.03NaNbO$_3$-xBaTiO$_3$ ($x = 0$, 0.01, 0.02, 0.04, 0.05, 0.06, 0.08) are synthesized using conventional solid state reaction method. Influence of BaTiO$_3$ on crystal structure, dielectric and piezoelectric properties are investigated. All compositions can form single perovskite phase. Powder x-ray diffraction patterns can be indexed assuming a pseudo-cubic structure. Lattice constant increases with the increase of BaTiO$_3$ concentration. Rhombohedral distortion is observed in poled samples with BaTiO$_3$ concentration up to 6 mol%. Temperature dependence of dielectric constant and dissipation factor measurement reveals that all compositions experience two phase transitions: from ferroelectric to antiferroelectric and from antiferroelectric to paraelectric. Both transition temperatures, T_c and T_f, are lowered due to introduction of BaTiO$_3$. Ferroelectric to antiferroelectric phase transition has relaxor characteristics. Piezoelectric properties have relatively higher value around 1 mol% to 4 mol% BaTiO$_3$. In ceramics with $x = 0.02$, thickness electromechanical coupling factor (k_t) of 0.51 and piezoelectric charge constant (d_{33}) of 110×10^{-12} C/N are obtained. Addition of small amount of BaTiO$_3$ ($x = 0.01$, 0.02) improves piezoelectric properties compared to NBT-NN binary system, while T_f remains above 140°C, higher than that of NBT-BT binary system composition with similar piezoelectric properties. This is in favor of the possible application of them as lead-free piezoelectric ceramics. © *2003 Kluwer Academic Publishers*

1. Introduction

Currently, piezoelectric ceramics based on lead zirconate titanate (PZT) system dominate piezoelectric ceramic applications. In processing, careful measure is required to avoid lead pollution. Besides, piezoelectric components may cause continuous damage to environment after they are abandoned. There is an increasing interest of the research and development of lead-free piezoelectric ceramics. Sodium bismuth titanate, (Na$_{1/2}$Bi$_{1/2}$)TiO$_3$, (abbreviated as NBT), is considered to be a candidate as lead-free piezoelectric ceramics [1–5]. NBT has a remanent polarization of 38 μC/cm^2 and a coercive field (E_c) of 73 kV/cm. At room temperature, NBT has rhombohedral symmetry. This ferroelectric phase transform to antiferroelectric tetragonal phase around 220°C. Antiferroelectric to paraelectric (tetragonal) phase transition occurs at about 320°C, resulting in maximum dielectric constant. Above 520°C, NBT is in cubic phase. It is difficult to pole NBT ceramics due to its large E_c. To improve its properties, solid solution of NBT with BaTiO$_3$ (BT), SrTiO$_3$ (ST) have been investigated [1–3]. Lanthanum (La) was also introduced to modify NBT's properties [5].

Another approach is the introduction of antiferroelectric NaNbO$_3$ (abbreviated as NN) to form solid solution [4]. This is the strategy adopted in the development of PZT, where PbTiO$_3$ is ferroelectric and PbZrO$_3$ is antiferroelectric. X-ray diffraction data show that rhombohedral-orthorhombic morphotropic phase boundary exists at $x = 0.90$–0.92 in system $(1 - x)$ NBT-xNN. The coupling factor k_{33} reaches a maximum at $x = 0.03$ with a piezoelectric constant d_{33} of 71×10^{-12} C/N.

In this paper, we extend the binary systems NBT-NN and NBT-BT to ternary system NBT-NN-BT at fixed NN concentration. Influence of BT on crystal structure, dielectric and piezoelectric properties are investigated.

2. Experimental procedure

Reagent grade oxide or carbonate powders of Bi$_2$O$_3$, NaCO$_3$, TiO$_2$, BaCO$_3$, are used as starting materials. Compositions selected in this work can be expressed in a general formula, $(0.97 - x)$NBT-xBT-0.03NN with $x = 0.00$, 0.01, 0.02, 0.04, 0.05, 0.06, 0.08 (hereafter
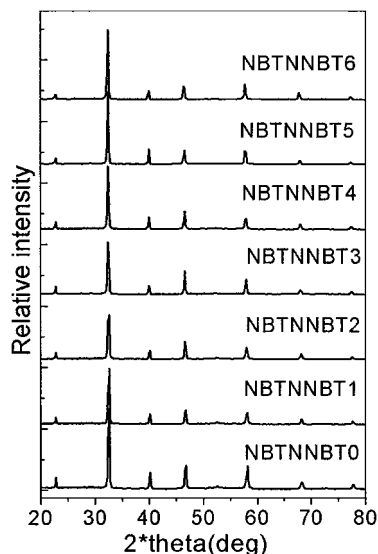
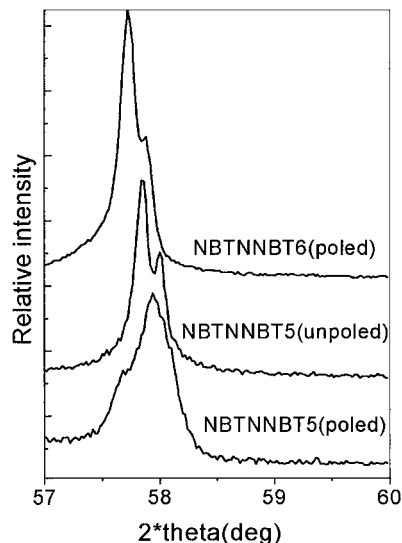*Figure 1* Powder XRD patterns at room temperature.

Figure 2 XRD patterns at room temperature of poled and unpoled samples at 2θ between $57°$ to $60°$.

named NBTNNBT0, NBTNNBT1, NBTNNBT2, NBTNNBT3, NBTNNBT4, NBTNNBT5, NBTNNBT6, respectively). All samples are prepared by the conventional ceramic procedure. Raw materials are mixed using planetary milling with ZrO_2 media and alcohol. The mixed powders are calcined at $820°C$ for 2 hours. The synthesized powders are then pelletized into disks of 20 mm in diameter and about 1.2 mm in thickness. After binder burnout, these pressed disks are sintered at $1180°C$ to $1200°C$ with two hours soaking period. Silver paste is fired on to sever as electrodes for electrical measurement. The ceramic bodies were poled in a silicon oil bath at temperature of $50°C$ with a DC field of 50 to 70 kV/cm for 5 minutes.

The lattice parameters are determined by x-ray powder diffraction (XRD) using Cu K_α radiation. Silicon is used as an internal standard for calibration. Lattice distortion is measured on poled samples in the 2θ range of $45°$ to $48°$, $57°$ to $60°$, and $75°$ to $79°$, corresponding to diffraction peaks of (200), (211), (310) planes, respectively, with respect to the rhombohedral axes. The dielectric constant and dissipation factor ($\tan \delta$) at room and elevated temperature are measured at 0.1 KHz, 1 KHz and 100 KHz using a LRC meter. The thickness electromechanical coupling factor (K_t) is determined using resonance method. The piezoelectric charge constant (d_{33}) is measured using a piezo-d_{33} meter at a frequence of 100 Hz.

Figure 3 XRD patterns at room temperature of poled and unpoled samples at 2θ between $75°$ to $79°$.

TABLE I Lattice constant and rhombohedral distortion

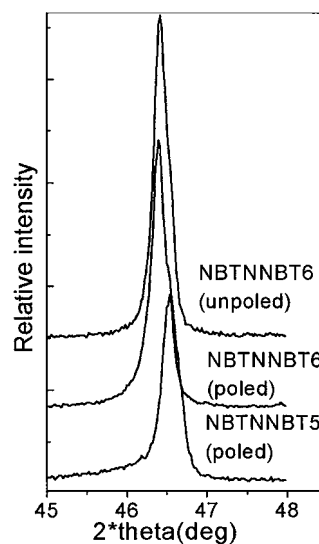| Sample no.	x	a (Å)	α (deg)
NBTNNBT0	0	3.8783(4)	89.71
NBTNNBT1	0.01	3.8902(4)	89.69
NBTNNBT2	0.02	3.8903(4)	89.80
NBTNNBT3	0.04	3.8952(4)	89.79
NBTNNBT4	0.05	3.8990(2)	89.69
NBTNNBT5	0.06	3.9024(2)	89.78
NBTNNBT6	0.08	3.9067(2)	–

Figure 4 XRD patterns at room temperature of poled and unpoled samples at 2θ between $45°$ to $48°$.
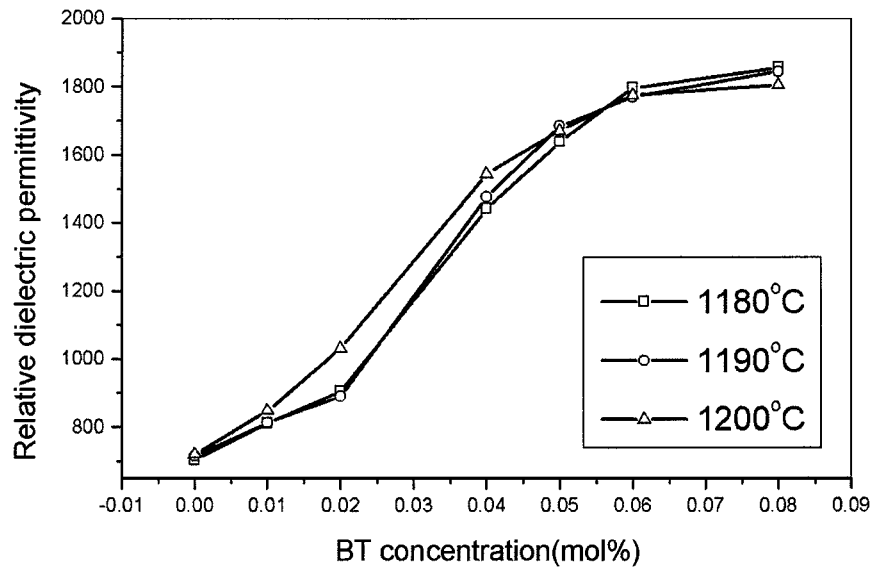
Figure 5 Relation between relative dielectric permittivity at 25°C and BT concentration of samples sintered at different temperatures. Measurement frequency is 1 kHz.
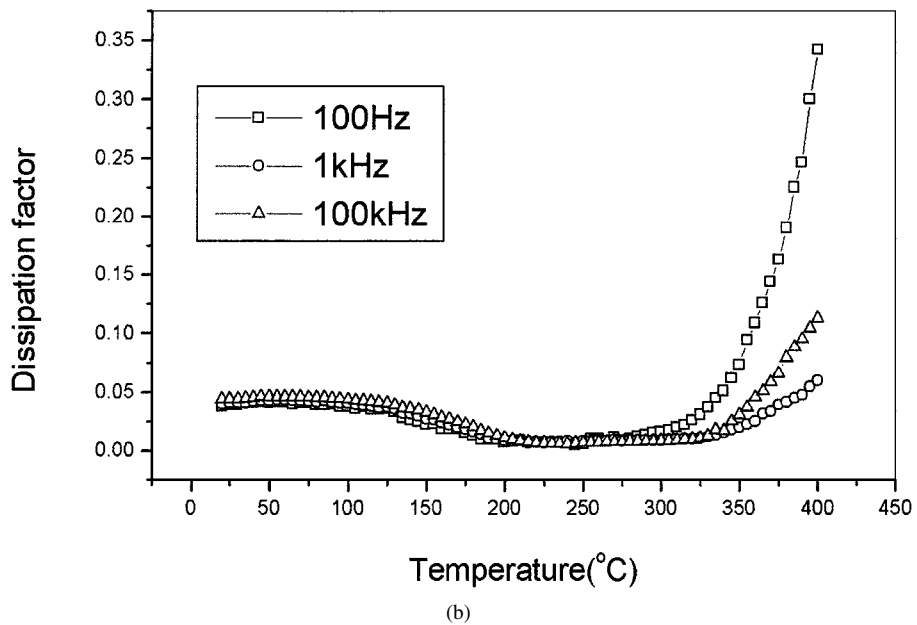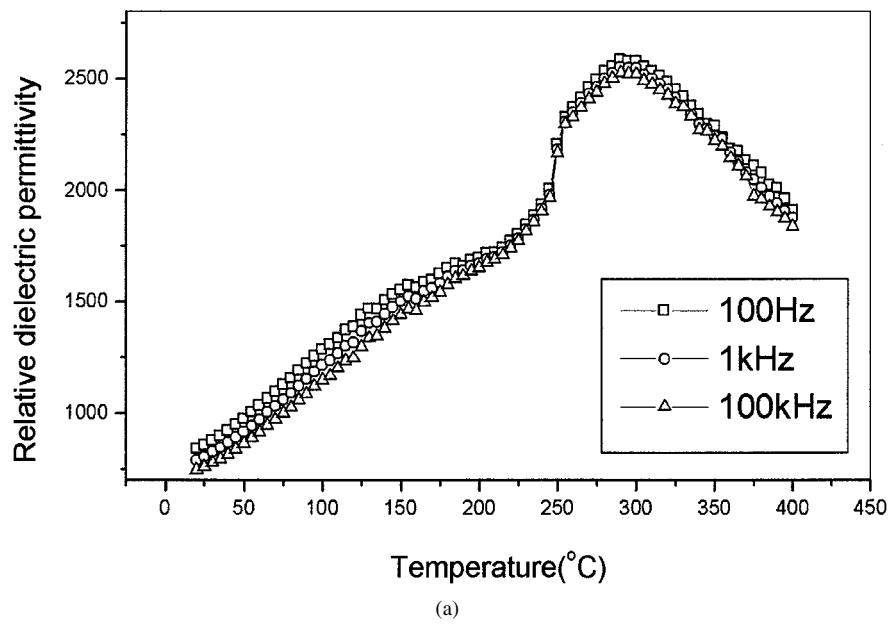

(a)

(b)

Figure 6 Change of (a) the relative dielectric permittivity and (b) dissipation factor with temperature and frequency of NBTNNBT1.

3. Results an discussion

3.1. Crystal structure

It is confirmed by XRD that single perovskite phase formed in all samples (Fig. 1). All diffraction patterns can be indexed assuming a pseudo-cubic structure. Lattice parameters obtained this way increase with the increase of BT concentration (Table I). To determine the lattice distortion in NBTNNBT compounds, poled samples are subject to XRD examination (Figs 2 and 3). The indices (hkl) of the reflecting planes in these two 2θ regions are (211) and (21$\bar{1}$), (310) and (3$\bar{1}$0) respect to rhombohedral axes, respectively. It is evident that all samples except NBTNNBT6 have rhombohedral distortion similar to pure NBT. These XRD peaks are used to calculate the lattice angle α (Table I). No rhombohedral distortion is observed in poled NBTNNBT6 sample. It was reported that a rhombohedral-tetragonal morphotropic phase boundary (MPB) exists in NBT-BT

binary system at about 6 mol% to 7 mol% BT [3]. In present work, BT concentration in NBTNNBT6 is greater than 6 mol%. We further exam NBTNNBT6 and NBTNNBT5 samples after poling procedure by XRD in 2θ range from 45° to 48°, corresponding to (200) plane of pseudo-cubic structure (Fig. 4). No peak split related to tetragonal distortion is observed.

It was reported that lattice distortion can be detected only after poling in La-doped NBT [5] and NBT-PbTiO$_3$ binary system [6]. This phenomenon can be attributed to the transition of ferroelectric microdomain to macrodomain under electric field. Such a transition is associated with relaxor ferroelectric behaviour, most obvious in Pb(Mg$_{1/3}$Nb$_{2/3}$)O$_3$, Pb(Zn$_{1/3}$Nb$_{2/3}$)O$_3$, etc, which have two kinds of ions of different valance at B-site of perovskite structure. The coexistence of Bi^{3+} and Na$^+$ ions at A site may also results in ferroelectric microdomain which is too
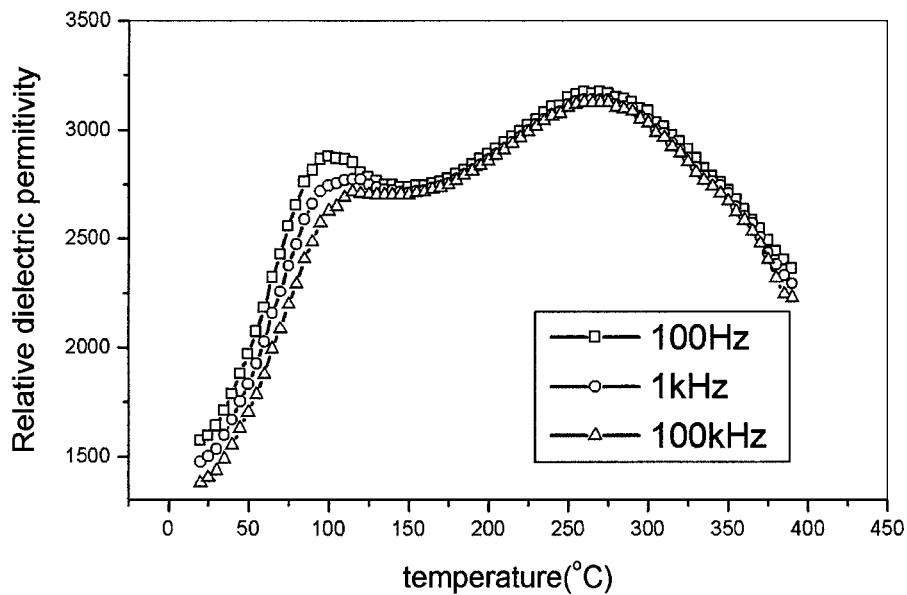
(a)
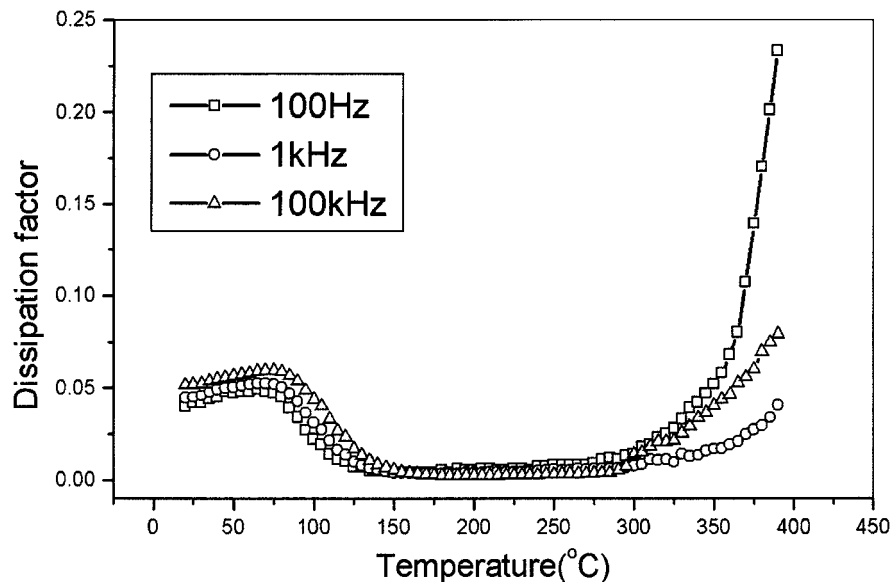
(b)

Figure 7 Change of (a) the relative dielectric permittivity and (b) dissipation factor with temperature and frequency of NBTNNBT3.

small to be detected by XRD technique and manifests itself only after effective poling. Introduction of Ba^{2+} and Nb^{5+} ions may further randomize the crystal structure, especially when their concentration is high.

3.2. Dielectric property

Relative dielectric permittivity at room temperature increases with the increase of BT concentration (Fig. 5). The temperature dependences of relative dielectric permittivity show maximum values, corresponding to antiferroelectric to paraelectric phase transition (Figs 6–9). This temperature, T_c, is lowered as the concentration of BT increases (Fig. 10). At lower BT concentration ($x = 0, 0.01, 0.02$), there are obscure bump around 200°C on relative dielectric permittivity vs. temperature curves (Fig. 6a). Such bumps were also reported in pure NBT [7], NBT-NN [4], NBT-PbTiO$_3$ [6] samples.

This can be regarded as the manifestation of the phase transition between ferroelectric and antiferroelectric phases. As BT concentration becomes higher, this obscure bump evolves into distinct hump [Figs 7–9]. Judged from these curves, the ferroelectric to antiferroelectric phase transition has relaxor characteristics, i.e. both dielectric permittivity and transition temperature, T_f, are strongly measurement-frequency dependent: the higher the frequency, the lower the permittivity value, and the higher the transition temperature. It is worthy to note that no clear relaxor behavior is observed at antiferroelectric to paraelectric phase transition. T_c and T_f measured at 1 kHz are given in Fig. 10. Both T_c and T_f decrease as BT concentration increases. At $x = 0.06$, T_f is as low as 115°C, and the appropriate operating temperature range for corresponding piezoelectric components will be limited.

All samples show similar dissipation factor behavior. Dielectric loss reaches minimum after ferroelectric
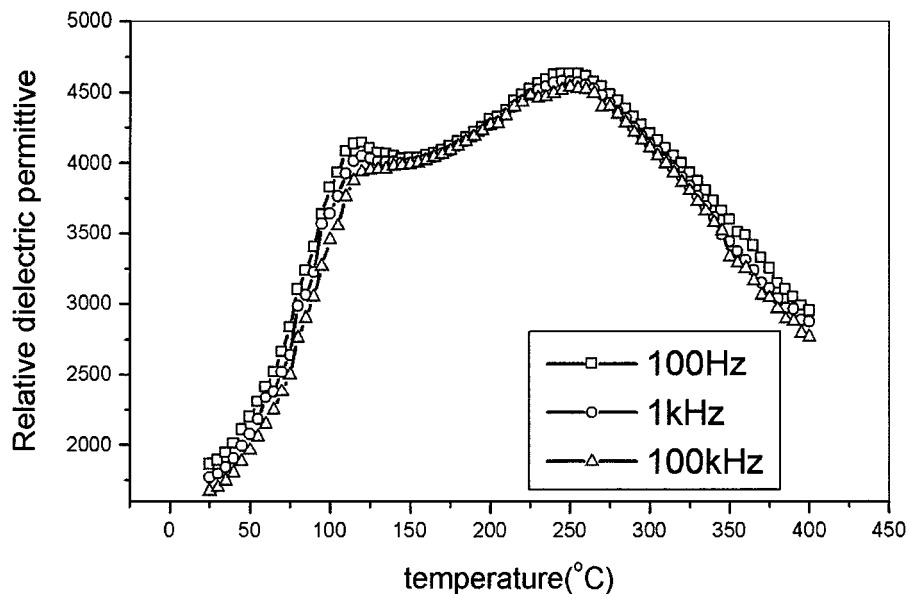
(a)
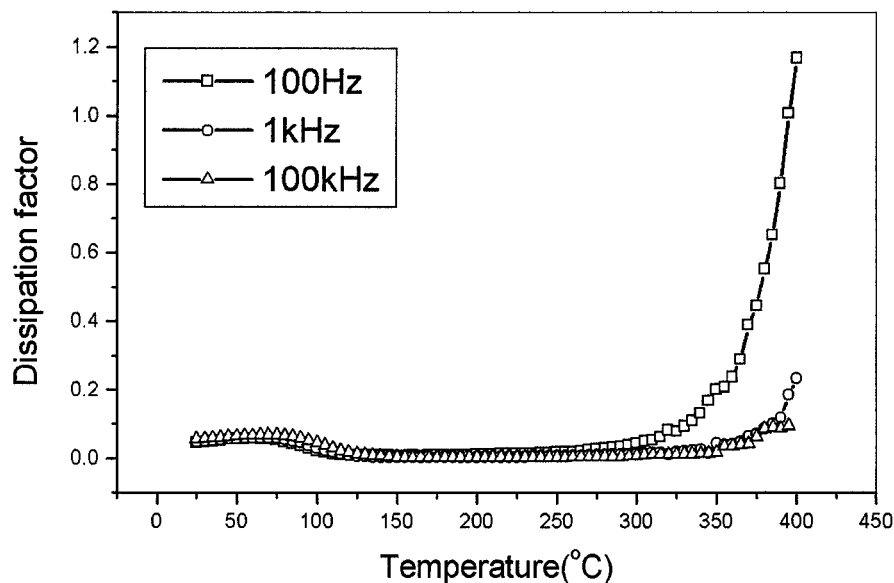
(b)

Figure 8 Change of (a) the relative dielectric permittivity and (b) dissipation factor with temperature and frequency of NBTNNBT5.
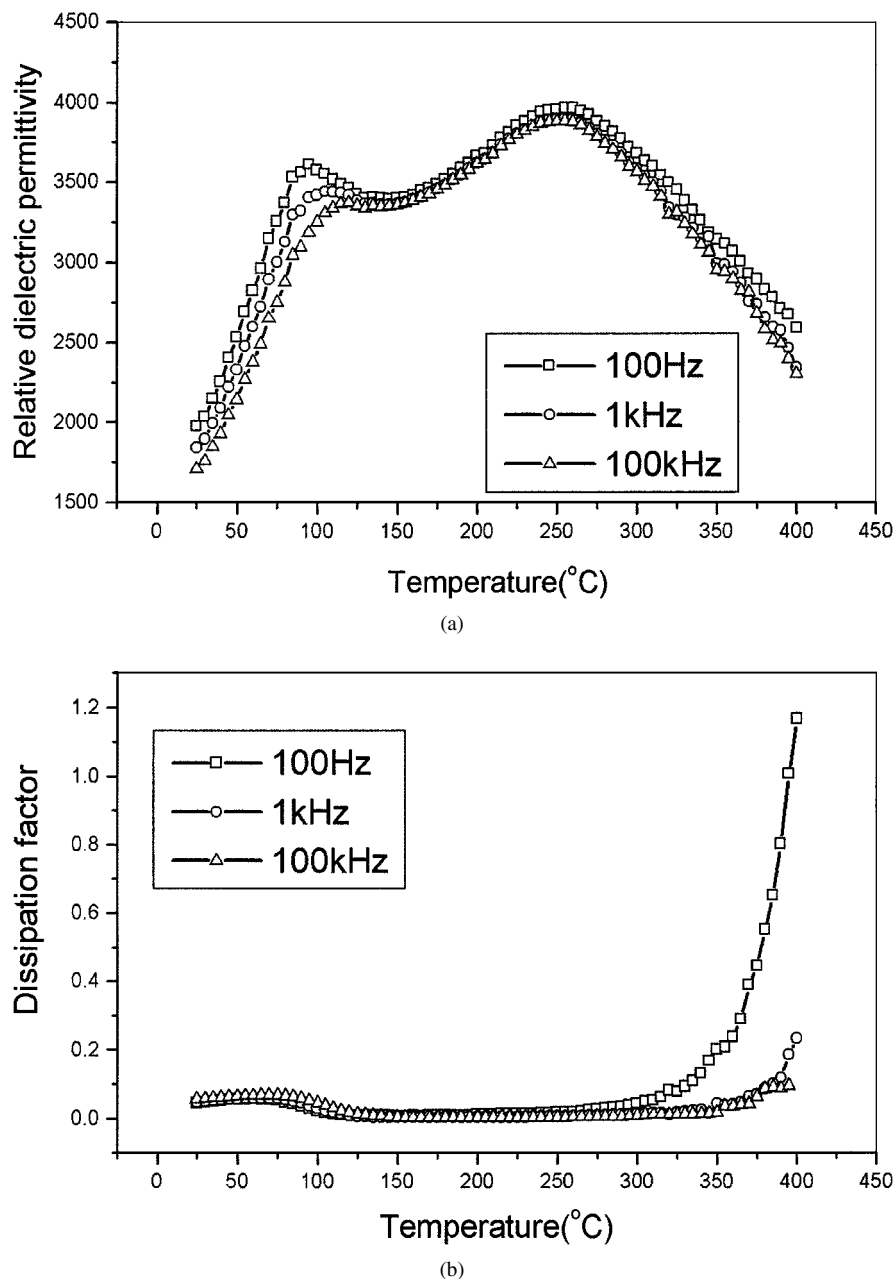
Figure 9 Change of (a) the relative dielectric permittivity and (b) dissipation factor with temperature and frequency of NBTNNBT6.

to antiferroelectric phase transition (Figs 6–9). At still higher temperature, it increases sharply. When antiferroelectric phase formed, ferroelectric domain wall's contribution to dielectric loss diminishes. Above T_c, electrical conductivity begins to dominate, resulting in an increase of the dissipation factor [8].

3.3. Piezoelectric property

Piezoelectric properties have relatively higher value around 1 mol% to 4 mol% BT (Figs 11 and 12). As mentioned above, appropriate operating temperature range of NBT based piezoelectric components is limited by T_f but not T_c. Compared to NBT-NN binary system [4], addition of small amount of BT ($x = 0.01$, 0.02) improves piezoelectric properties, while T_f remains above $140°C$. Although similar piezoelectric properties can be obtained in composition of 0.94NBT-0.06BT [3], its T_f (below $110°C$) is significantly lower than NBTNNBT1

and NBTNNBT2. According to present work, composition NBTNNBT1 and NBTNNBT2 which has relative higher d_{33}, k_t and T_f values may find their applications as lead-free piezoelectric ceramics.

No obvious piezoelectric effect is observed in composition NBTNNBT6, although it is considered to be in ferroelectric phase from dielectric permittivity measurement at both poling and room temperature. High BT concentration may results in a high disturbance of NBT crystal structure and forbids the electrical dipoles to form effective ferroelectric domain large and/or stable enough with or without electrical field, which is consistent with the XRD observation (Figs 2, 4). It is necessary to prepare samples with still higher BT concentrations and to employ other experimental technique, such as selected area electron diffraction at different temperatures, to elucidate the phase transition behavior of NBT-NN-BT ternary system in high BT concentration region.
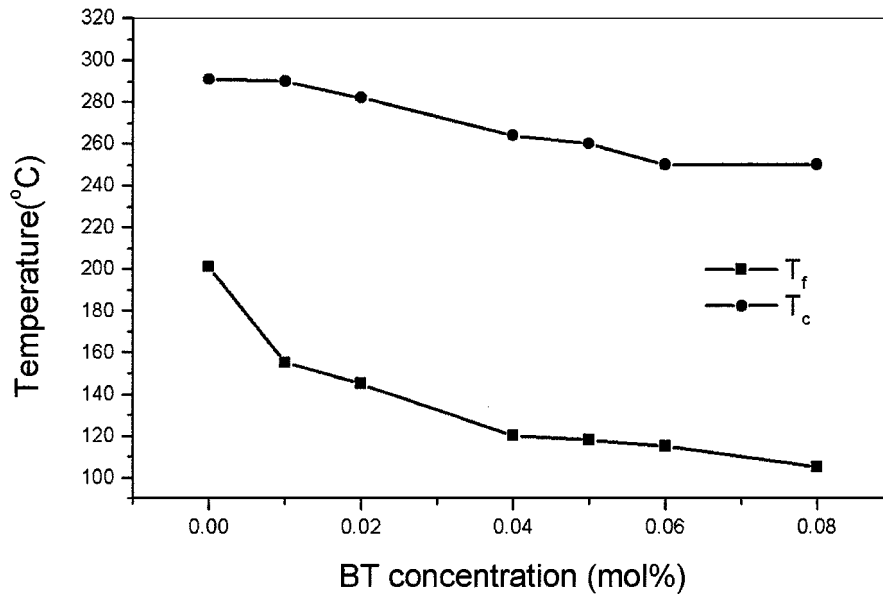
Figure 10 Change of phase transition temperature (a) T_c and (b) T_f with BT concentration.
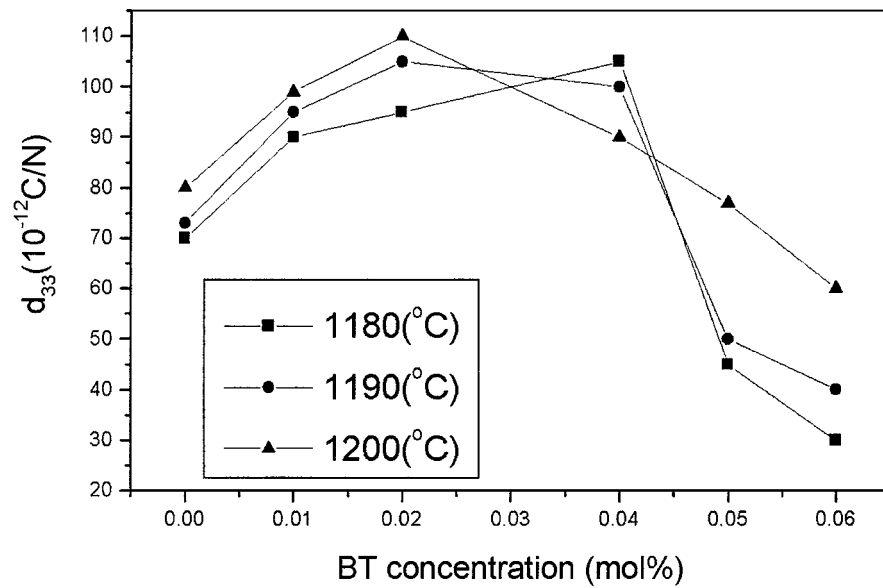

Figure 11 Relation between piezoelectric charge constant d_{33} at 25°C and BT concentration of samples sintered at different temperatures.
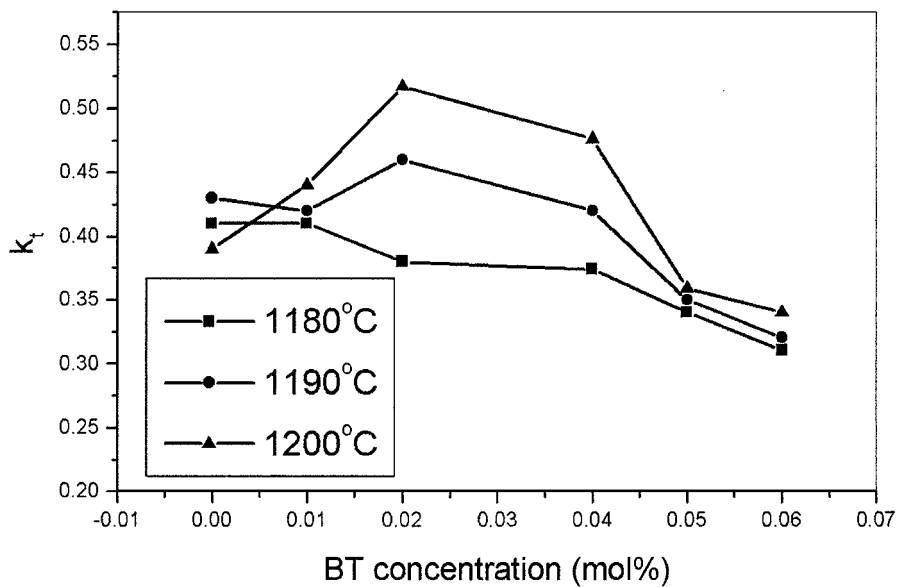

Figure 12 Relation between thickness electromechanical coupling factor k_t at 25°C and BT concentration of samples sintered at different temperatures.

4. Conclusion

All compositions investigated in present work can form single perovskite phase. Powder x-ray diffraction patterns can be indexed assuming a pseudo-cubic structure. Lattice constant increases with the increase of BT concentration. Rhombohedral distortion is observed in poled samples with BT concentration up to 6 mol%. From room temperature to 450°C, all compositions experience two phase transitions: from ferroelectric to antiferroelectric and from antiferroelectric to paraelectric. Both transition temperatures are lowered due to introduction of BT. Ferroelectric to antiferroelectric phase transition has relaxor characteristics. Piezoelectric properties have relatively higher value around 1 mol% to 4 mol% BT. Addition of small amount of BT ($x = 0.01$, 0.02) improves piezoelectric properties compared to NBT-BT binary system, while T_f remains above 140°C, higher than that of NBT-BT binary system composition with similar piezoelectric properties. This is in favor of the possible application of them as lead-free piezoelectric ceramics.

References

1. T. TAKENAKA and K. SAKATA, *Ferroelectrics* **95** (1989) 153.
2. T. TAKENAKA, K. SAKATA and K. TODA, *ibid.* **106** (1990) 375.
3. T. TAKENAKA, K. MARUYAMA and K. SAKATA, *Jap. J. App. Phy.* **30B** (1991) 2236.
4. T. TAKENAKA, T. OKUDA and K. TAKEGAHARA, *Ferroelectrics* **196** (1997) 175.
5. A. HERABUT and A. SAFARI, *J. Amer. Ceram. Soc.* **80** (1997) 2954.
6. S. KUHARUANGRONG and W. SCHULZ, *ibid.* **79** (1990) 1273.
7. S. SAID and J. MERCURIO, *J. Euro. Ceram. Soc.* **21** (2001) 1333.
8. S. KUHARUANGRONG, *J. Mater. Sci.* **36** (2001) 1727.